Water Desalination using Capacitive Deionization with Microporous Carbon Electrodes

S. Porada,[1,2,*] L. Weinstein,[3] R. Dash,[3] A. van der Wal,[4,5] M. Bryjak,[1] Y. Gogotsi,[6] P.M. Biesheuvel[2,4]

[1]*Department of Polymers and Carbon Materials, Faculty of Chemistry, Wroclaw University of Technology, Wybrzeze Wyspianskiego 27, 50-370 Wroclaw, Poland*. [2]*Wetsus, centre of excellence for sustainable water technology, Agora 1, 8934 CJ Leeuwarden, The Netherlands.* [3]*Y-Carbon, Inc., 900 First Ave, King of Prussia, PA 19406 , USA.* [4]*Department of Environmental Technology, Wageningen University, Bornse Weilanden 9, 6708 WG Wageningen, The Netherlands*. [5]*Voltea B.V., Wasbeekerlaan 24, 2171 AE Sassenheim, the Netherlands.* [6]*Department of Materials Science and Engineering, Drexel University, Philadelphia, PA 19104, USA.*

Abstract

Capacitive deionization (CDI) is a water desalination technology in which salt ions are removed from brackish water by flowing through a spacer channel with porous electrodes on each side. Upon applying a voltage difference between the two electrodes, cations move to and are accumulated in electrostatic double layers inside the negatively charged cathode and the anions are removed by the positively charged anode. One of the key parameters for commercial realization of CDI is the salt adsorption capacity of the electrodes. State-of-the-art electrode materials are based on porous activated carbon particles or carbon aerogels. Here we report the use for CDI of carbide-derived carbon (CDC), a porous material with well-defined and tunable pore sizes in the sub-nanometer range. When comparing electrodes made with CDC with electrodes based on activated carbon, we find a significantly higher salt adsorption capacity in the relevant cell voltage window of 1.2-1.4 V. The measured adsorption capacity for four materials tested negatively correlates with known metrics for pore structure of the carbon powders such as total pore volume and BET-area, but is positively correlated with the volume of pores of sizes <1 nm, suggesting the relevance of these sub-nm pores for ion adsorption. The charge efficiency, being the ratio of equilibrium salt adsorption over charge, does not depend much on the type of material, indicating that materials that have been identified for high charge storage capacity, can also be highly suitable for CDI. This work shows the potential of materials with well-defined sub-nanometer pore sizes for energy-efficient water desalination.

KEYWORDS: capacitive deionization; carbide-derived carbons; water desalination; electrostatic double layer theory; porous electrodes; millifluidics

1. Introduction

Many regions in the world suffer from brackish ground water and increasing salinity levels, a trend which is expected to continue, affecting the lives of billions of people.[1-8] Reverse osmosis (RO) and thermal processes are the currently used technologies for large-scale water desalination.[9] In these approaches, desalted water is produced from sea or brackish water either by passing water through water-permeable membranes under pressure, or by distillation, respectively. However, in those processes, where desalted water is removed from the feed water, energy consumption is inherently significant. For instance, for an energy consumption in RO of 4 kWh per m^3 of fresh water produced from sea water, operation is at about 4x the thermodynamic minimum (water recovery=0.6, $c_{salt,sea}$=0.5 M).[5,10] It is not unreasonable to assume that for brackish water of relatively low ionic strength it is energetically favorable to remove the salt ions instead of the water.

Technologies where ions are removed from water by electrical fields include electro-deionization and electrodialysis,[11,12] water desalination using microchannels[13] and batteries,[14] and capacitive deionization (CDI).[8,10,15-27] In the present work we focus on CDI. Capacitive deionization (CDI) is a milliffluidic water desalination technology in which the salt ions in brackish water are removed by flowing the water through a spacer channel with porous electrodes on each side. Upon applying a potential difference between the two electrodes, cations (Na^+) move to and are accumulated in the cathode, and anions (Cl^-) are absorbed by the anode. In this way, partially desalted water is obtained. After some time, the voltage is reduced, or even reversed, and ions are released from the electrodes, leading to a concentrated salt product stream which is discharged. Note that reversal of voltage is only possible when also ion-exchange membranes are used between the electrodes and the spacer in a modification of CDI, called membrane-CDI.[28-33]

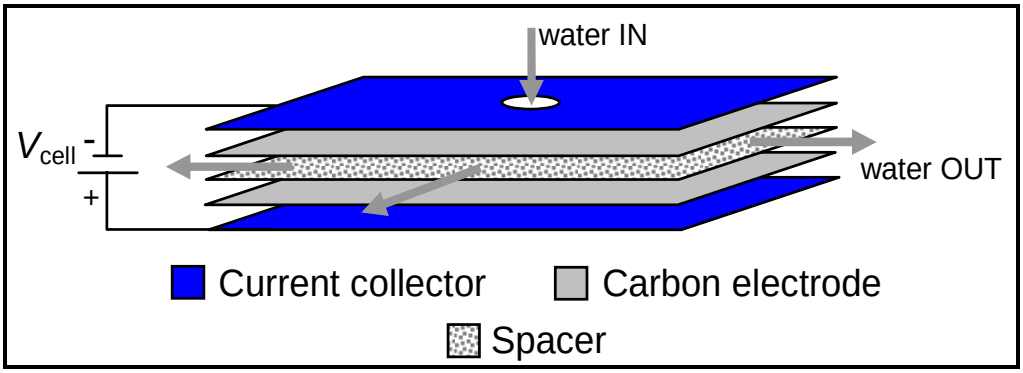

Fig. 1. Schematic view of a capacitive deionization cell. Influenced by the electrical field, cations present in the water flowing through the spacer channel migrate into the negatively charged porous carbon electrode (cathode); simultaneously, anions migrate into the anode.

One of the key parameters for commercial realization of CDI is the salt adsorption capacity of the electrodes, which determines the amount of ions which can be stored inside the pores of the carbon electrode. Traditionally, electrodes for water treatment have been based on carbon aerogels,[34,35,36] porous activated carbons,[37] and carbon cloth.[38,39] More recently graphene,[40] carbon nanotubes[41] and carbon nanotubes/nanofibre-mixtures were used for CDI.[42]

Porous activated carbons are characterized by a high internal surface area and porosity, but conventional methods of producing carbons from organic precursors do not offer sufficient control over the porosity, typically leading to a wide distribution of pores ranging from micro (< 2 nm) to macropores (> 50 nm). By using those materials it may be difficult to find the exact effect of the pore size on ion removal ability in water desalination. Materials of which the porosity can be controlled on the atomic level are required for such a study. Here we report on the highly promising salt adsorption capacity of an inorganic porous material with such high control of pore size, namely carbide-derived carbon (CDC). This result confirms the potential of CDC electrodes for energy-efficient water desalination and exemplifies the ability to optimize tunable nanoporous carbon materials for specific applications.

The synthesis of CDC is based on removing metal or metalloid atoms from metal carbide, such as silicon or titanium carbide, using an etchant, normally chlorine gas, leaving behind porous carbon. The pore size and structure in the carbon produced is dependent on the synthesis conditions and the selected carbide.[43] It has been shown that the pore size distribution is narrow and can be controlled

with sub-Ångstrom accuracy between 0.5 and 2.2 nm by selecting the precursor material (TiC, SiC, etc.) and the synthesis conditions.[43] This level of control is unattainable using conventional carbon synthesis techniques. Furthermore, the process can be readily scaled up to large-scale continuous manufacturing, as has been demonstrated by an industrial member of the research team (Y-Carbon). The raw materials used are commercially available and relatively inexpensive. Because of the well-defined pore size control in the sub-nanometer range, CDC-based electrodes have very large charge storage capacities in organic solvent for supercapacitor applications.[44,45] Other promising applications for CDC-based materials are as sorbents for the storage of hydrogen, methane[43] and carbon dioxide.[46] In this paper, we report for the first time the use of CDC-based electrodes in a CDI set-up for the removal of NaCl from water.

2. Experimental

Powders

Porous carbon materials used in this study include two commercially available activated carbon powders (YP50-F, Kuraray Chemical Osaka, Japan; DLC-Super 50, Norit, Netherlands), as well as two types of carbide-derived carbons with very narrow pore size distributions in the range of 7 Å to 20 Å (Y-Carbon, Inc., USA, www.Y-Carbon.US). These four materials will be referred to as AC-1, AC-2, CDC-1 and CDC-2, respectively. The CDC materials were synthesized from a carbide precursor by a chlorination process.[47] In this process metal atoms are selectively extracted from the carbide, with a pure carbon porous matrix remaining. The CDC primary pore size is 7.5 Å for both materials, but CDC-1 has relatively more of these primary pores than CDC-2, with a cut-off close to 1 nm. The pore structures of all materials were analyzed by adsorption/desorption of Argon at 77 K (liquid nitrogen temperature) using an ASAP 2020 Physisorption Analyzer (Micromeritics, Norcross, GA). Argon sorption analysis was used for calculating SSA using the Brunauer-Emmet-Teller (BET) equation for Specific Surface Area (SSA) and non-local density functional theory (NLDFT) to determine total pore volume, and the volume of pores less than 1 nm. While we used BET to calculate SSA in this work, DFT SSA gives a similar result for CDC.[44] Pore size distributions and pore volumes were determined using the NLDFT method provided by Micromeritics ASAP version 3.04 for finite slit-shaped pores in carbon.[48] The parameters of the porous structure calculated based on the corresponding isotherms are shown in Fig. 2a. For all powders we measured that the particle size is of the order of a few microns.

Electrode synthesis

All electrodes were prepared using the same procedure. First, a carbon slurry was prepared by adding 85 wt% of porous carbon material, 5 wt% of carbon black and 10 wt% of polyvinylidene fluoride (PVDF) to N-methyl-2-pyrrolidone with a 30:1 NMP:PVDF weight ratio. After intensive mixing, the slurry was deairated and stored at 50 ^{o}C for 24 h to obtain a homogeneous mixture. Then carbon electrodes were prepared by casting directly on a glass plate (slit height of casting knife 500 µm), followed by immersion in deionized water to solidify the binder.[49] Before the CDI experiments were performed, the carbon electrodes were cut into square pieces of 6x6 cm^2 with a hole in the middle of each electrode of 1.5x1.5 cm^2. Thus, the electrode area A is 33.8 cm^2 (that is, the area of the spacer channel covered by the porous electrode, either anode or cathode). The electrode manufacturing results in small differences in the average electrode mass per unit area, m_{area}: for AC-1 we obtain m_{area}=160 g/m^2, for AC-2 167 g/m^2, for CDC-1 132 g/m^2, and for CDC-2 173 g/m^2.

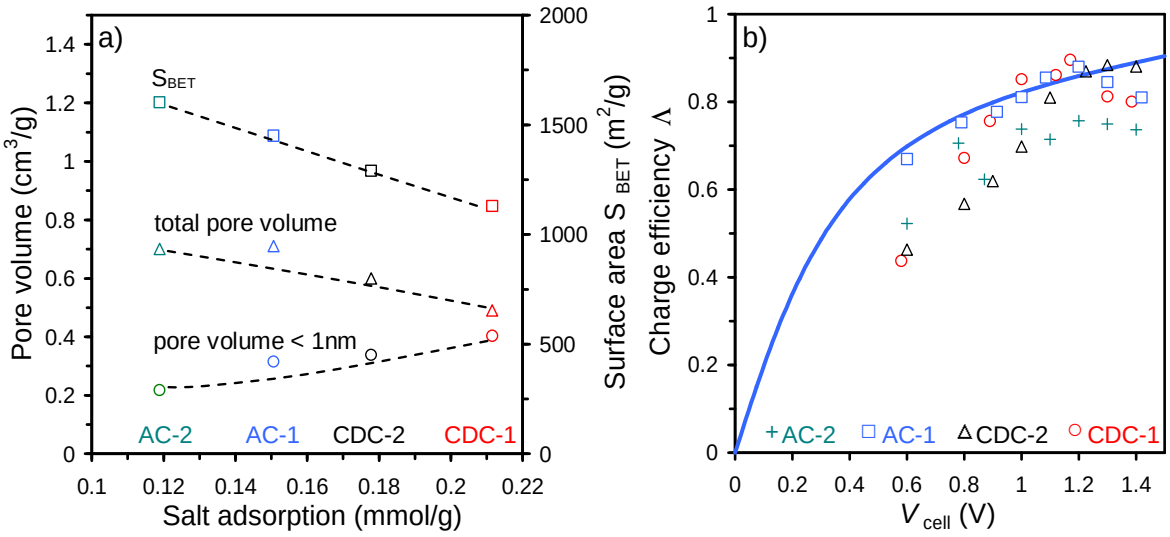

Fig. 2. Data for the four tested materials of (a) Correlation between salt adsorption capacity (x-axis), BET surface area (S_{BET}, squares, right y-axis), total pore volume (triangles, left y-axis), and pore volume in the size range < 1 nm (circles, left y-axis) at V_{cell}=1.2 V, c_{salt}=5 mM; (b) Charge efficiency Λ as function of cell voltage at c_{salt}=5 mM. Line is based on the modified Donnan model.

CDI-experiments

Experimental details of our CDI test system have been described in refs. 27 and 32. A "stack" consisting of N=8 parallel cells as depicted in Fig. 1 is assembled from current collectors, electrodes, and spacers. To ensure symmetry in each cell, electrodes were weighted and matched in pairs of equal mass before putting the stack together. Each current collector is used for two adjacent cells (one above, and one below). Materials are graphite current collectors, porous carbon electrodes made from AC-1, AC-2, CDC-1 and CDC-2 powders, and a porous spacer (Glass fibre prefilter, Millipore, Ireland, uncompressed thickness δ_{sp}=350 µm). After assembly of all materials, the entire stack of all layers is firmly pressed together, placed in a rectangular teflon housing filled with water, and sealed. During operation, the flow of salt solution through the stack is held constant at Φ=1 mL/s. The solution flows from the center hole radially outward through the N spacer layers, and leaves these square layers on all four sides, entering into a small volume of "dead space" surrounding the stack before flowing out of

the housing via a plastic tube to a conductivity meter placed in-line. At the start of the ion adsorption step, a positive cell voltage V_{cell} (the voltage between anode and cathode) is applied using a power supply. At the start of the desorption step, the cell voltage is reduced to zero.

The effluent salt concentration, c_{eff}, as plotted in Fig. 3a, is calculated from the measured conductivity, and the equilibrium salt removal, Γ_{salt}, see Fig. 4a, is derived by integrating the difference between inflow (c_{in}) and outflow concentration (c_{eff}) over time, multiplying by the flow rate Φ and dividing by m_{tot}. The total electrode mass in the stack, m_{tot}, is equal to $m_{tot}=m_{area}*2*N*A$. For each experiment (each experimental point in Fig. 4), the adsorption/desorption cycle (Fig. 2) was repeated several times until the cycle becomes the same as the previous one (the traces of current vs time, and of c_{eff} vs time have become the same as the previous one). This situation we call the "dynamic steady state" (DSS) and the data presented are obtained in the DSS. Both experimentally and theoretically, when the DSS is reached, the salt removal during the ion adsorption-step is equal to the release of salt in the desorption-step, and likewise for charge (except for a small leakage current). The electrical current from cathode to the anode is plotted as function of time in Fig. 3b as a current density, i.e., the total current divided by the stack electrode area, which is $N*A$. The current during the ion desorption step is integrated with time and divided by the total electrode mass in the stack, m_{tot}, to obtain the charge Σ_F expressed in C/g plotted in Fig. 4b.

All experiments were done using a c_{in}=5 mM NaCl-solution (290 ppm, 550 μS/cm). The pH of the feed solution was maintained constant at pH 7.5 by automatic addition of small amounts of 0.1 M hydrochloric acid or 0.1 M sodium hydroxide to the 10-liter storage vessel from which the CDI-stack was fed and to which the effluent was returned. The vessel is continuously flushed with N_2 gas to purge the water from dissolved oxygen.

3. Results & Discussion

In this section we present results for salt adsorption and charge for CDI using four types of electrodes, two based on activated carbons, AC, and two based on carbide-derived carbons, CDC. Fig. 3a shows example data for the effluent salt concentration as function of time for two of the four types of electrodes. Fig. 3b shows the trace of current density vs. time for the same two experiments. Though in the experiment both the adsorption and desorption steps take 1500 s, here only data for the first 1000 s of each step is shown, because the final 500 s of each step only show minor changes.

Fig. 3a shows that during the ion adsorption step, after a step-change in cell voltage to V_{cell}=1.2 V is applied between the two electrodes, the salt concentration in the effluent water decreases rapidly reaching a minimum, after which the concentration increases again because the salt adsorption capacity of the electrode pair is slowly reached. Short-circuiting the cell at the start of the desorption step leads to rapid ion release from the electrodes and a sudden increase in the effluent salt concentration. The integrated area of each curve (limited by the line "concentration=5 mM") relates to the total salt removal by the electrode pairs as plotted in Fig. 4a. Fig. 3a shows how the CDC-2 material adsorbs and releases salt somewhat more slowly than AC-1, possibly due to the smaller pore size, but as we will show next, the maximum, or equilibrium, adsorption is actually higher.

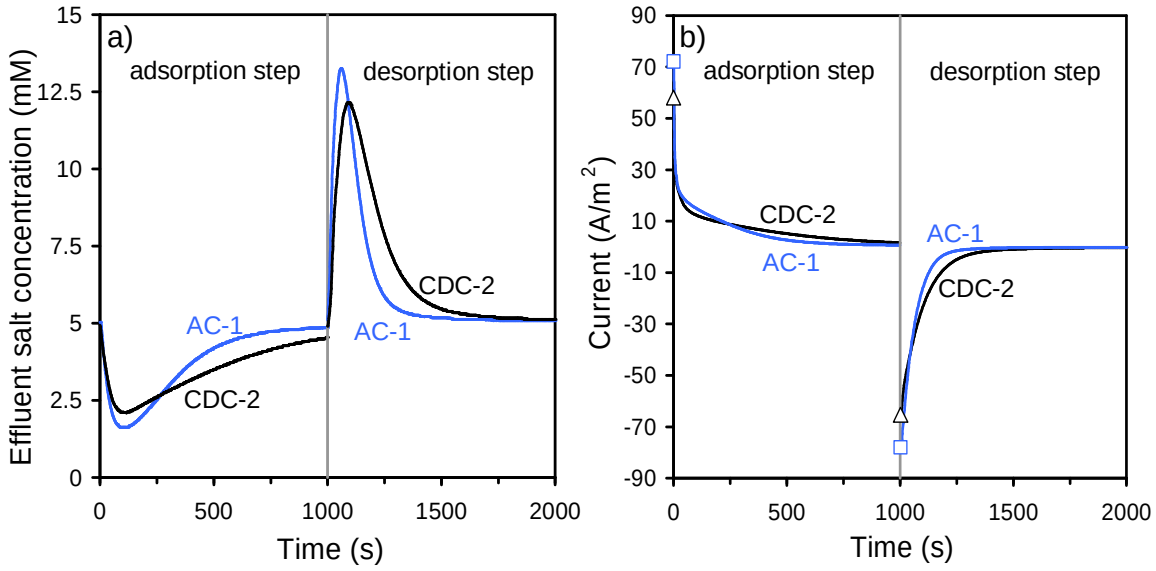

Fig. 3. Data for (a) Effluent salt concentration and (b) current density, as function of time in CDI during ion adsorption and desorption, for AC-1 and CDC-2 electrodes (V_{cell}=1.2 V, c_{in}=5 mM).

The duration of the salt adsorption/desorption cycle is 1500 s, both for the ion adsorption step and for the ion desorption step. This time is sufficient for equilibrium to be reached. Equilibrium implies that ion transport rates have become zero and the applied cell voltage is completely built off in the EDLs in the carbon particles, and there are no longer concentration or voltage gradients in the transport pathways (interparticle porosity) within the electrode or in the spacer channel. Fig. 4a shows data for the equilibrium salt adsorption as function of cell voltage, for all four carbon materials tested. Comparing AC-1 and AC-2 to CDC-2, we see that for V_{cell}=1.2 V CDC-2 has a higher salt removal than AC-1 by ~15% and when compared with AC-2 by ~33%. The difference in salt removal increases to ~18% and ~35% respectively when the cell voltage is increased to 1.4 V. Using CDC-1 the salt removal is even higher, up to ~28% higher than for AC-1 and up to ~44% for AC-2 both for V_{cell}=1.2 V and 1.4 V. For charge we observe similar differences, with a 23% and 34% increase relative to AC-2 and with a 15% and 27% increase relative to AC-1 at V_{cell}=1.2 V for CDC-2 and CDC-1, respectively.

Next we analyze data for charge efficiency, Λ, the ratio between the equilibrium salt adsorption, Γ_{salt}, and charge, Σ_F divided by Faraday's constant, F, see Eq. 4 below. Charge efficiency[17,18,27,50,51] is an important parameter because it quantifies how many 1:1 salt molecules are adsorbed for each electron transported from anode to cathode during the adsorption step, for the condition that equilibrium has been reached in the cell, and salt and charge flow into the electrode has therefore stopped. One should realize that Λ theoretically has to be <1 because simultaneously with counterion adsorption (the ions which are attracted into the EDLs during the salt removal step), also coions are depleted from the same electrode (coions are the ions that are expelled from the charged surface). This coion expulsion from the electrodes is the origin for the reduction of Λ to values below unity i.e., the phenomenon that for each electron transferred, less than one salt molecule is removed from the water flowing through the cell. To have high salt removal at a low input of electrical energy, it is therefore

very important to keep the value of Λ as close to unity as possible for a low cost desalination process based on CDI.

Fig. 2b shows data for Λ obtained from the equilibrium data for Γ_{salt} and Σ_F as presented in Fig. 4. The experimental data reach a plateau value of Λ~0.85 which is in good agreement with our previous findings described in ref. 27. It is interesting to note that the different structures of the materials tested (activated carbon and carbide-derived carbon) have relatively minor effects on the $\Lambda(V_{cell})$-curve. Certainly when considering only data above V_{cell}=1.0 V, and excluding data of material AC-2, we find that the three data sets for Λ closely overlap. If it can be established that this preliminary finding is a general feature of microporous carbon materials, this would imply that materials that are found to have high charge storage for supercapacitor applications, may also be highly suitable for application in CDI, i.e., a direct correlation exists between charge storage and salt adsorption capacity.

Indeed, as Fig. 4 shows, the sequence of materials with increasing charge storage capacity (AC-2 $\rightarrow$ AC-1 $\rightarrow$ CDC-2 $\rightarrow$ CDC-1) exactly matches the sequence for salt adsorption capacity. This also suggests that the same rationale that ascribes high charge storage capacity to the presences of sub-1nm-pores,[44] also applies to salt adsorption. And indeed, we find in Fig. 2a that the salt adsorption capacity (just like we we would find if we would plot charge on the x-axis here) positively depends on the volume of sub-1nm-pores, while it negatively depends on total pore volume or BET-area (all defined per gram of carbon). As Fig. 2a shows, the commercially available activated carbons AC-1 and AC-2 have a larger BET-surface area and also a larger total pore volume, but electrodes prepared from them have a lower salt adsorption capacity, when compared to the CDC-based electrodes. This is in contrast to the still prevailing view that the salt adsorption capacity would be proportional to the (BET) surface area within the electrodes, as classical double layer theory would suggest.

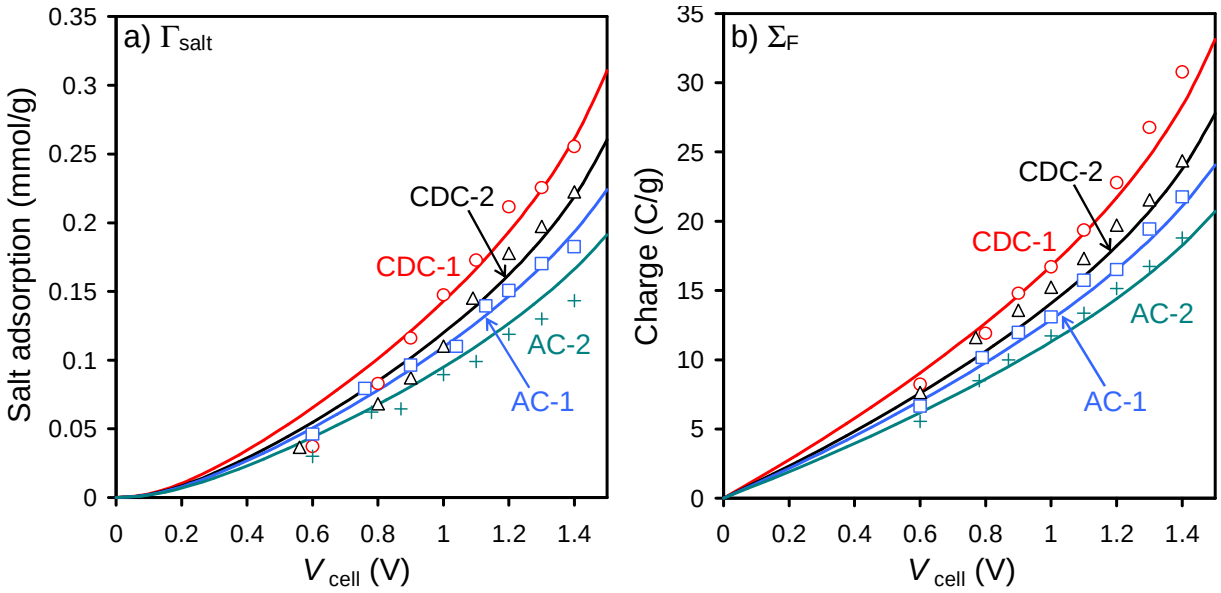

Fig. 4. (a). Equilibrium salt adsorption Γ_{salt} and (b). Equilibrium charge Σ_F, as function of cell voltage for CDC-1 (circles), CDC-2 (triangles), AC-1 (squares), and AC-2 (crosses). Salt concentration c_{in}=5 mM NaCl. Lines are fits using the modified Donnan model. Data given per gram of anode and cathode combined.

4. Modified Donnan model

In this section we present a modeling approach that can be used to fit data for equilibrium salt adsorption and charge in microporous electrodes, based on assuming that the electrical double layers (EDLs) inside the carbon particles are strongly overlapping. This is a valid assumption when the Debye length (a measure of the extension of the diffuse part of the double layer, ~3 nm for a 10 mM 1:1 salt solution) is much larger than the typical pore size. This assumption is well met for CDCs, where most ions are adsorbed in pores with diameters below 2 nm. In this limit, it is possible to make the "Donnan" assumption that the electrolyte inside the carbon particles has a constant electrical potential. Obviously this is an approximation of the detailed structure of the EDL in microporous carbons[52,53] but the Donnan approach has the advantage of being mathematically simple and fairly well fits data both for charge and salt adsorption.[32] Because of its compactness, it can be included in porous electrode mass transport theory.[54,55] To analyze the data, we make two modifications to the classical Donnan approach.[53] The first is to consider a dielectric capacity in between the location of the electron charge and the ions. The presence of this Stern layer reflects that the ion charge cannot come infinitely close to the electron charge, for instance due to the (hydrated or dehydrated) ion size, or because the electron charge is not exactly located at the edge of the carbon material, or because of an atomic "roughness" of the carbon/electrolyte interface. The second modification is to include a chemical attraction energy for the ion when it transfers from outside to inside the carbon particles, described by a term μ_{att}, i.e., there is an additional, non-electrostatic, attraction of the ion into the micropores.[56]

This "modified Donnan (mD) model" containing these two modifications, see refs. 32 and 55, is described by the following equations. First of all, the concentration of ion *j* in the pores inside the carbon particle is given by

$$c_{j,pore} = c_{salt,outside} \cdot \exp\left(-z_j \cdot \Delta\phi_d + \mu_{att}\right) \quad (1)$$

where z_j=+1 for the cation and z_j=-1 for the anion, while $\Delta\phi_d$ is the Donnan electrostatic potential difference between inside and outside the carbon particle.

The difference between $c_{cation,pore}$ and $c_{anion,pore}$ is the volumetric pore charge density, $c_{charge,pore}$, which relates to the Stern layer potential difference $\Delta\phi_{St}$ according to

$$c_{charge,pore} = c_{cation,pore} - c_{anion,pore} = -RT/F^2 \cdot \Delta\phi_{St} \cdot C_{St,vol} \quad (2)$$

where $C_{St,vol}$ is a volumetric Stern layer capacity. Likewise, we can define a total ion concentration as $c_{total\ ions,pore} = c_{cation,pore} + c_{anion,pore}$. To compare with experiment, we must recalculate pore concentrations to the measurable parameters of equilibrium charge Σ_F and salt adsorption Γ_{salt} (relative to the salt adsorption at zero applied voltage, i.e., at V_{cell}=0 V) as given by[32]

$$\Gamma_{salt} = \tfrac{1}{2} \cdot \upsilon \cdot \left(c_{total\ ions,pore} - c^0_{total\ ions,pore}\right) \ , \ \Sigma_F = -\tfrac{1}{2} \cdot F \cdot \upsilon \cdot c_{charge,pore} \quad (3)$$

where superscript "0" refers to the total ion adsorption at a cell voltage of V_{cell}=0 and where the parameter υ is the micropore volume per unit electrode mass (numbers given in Fig. 2a, to be multiplied by 0.85 to account for the mass fraction of carbon in the electrode). We can combine Eqs. 1-3 and derive that the charge efficiency, Λ, which is the ratio of equilibrium salt adsorption Γ_{salt} over charge Σ_F (divided by *F*) relates to the Donnan potential $\Delta\phi_d$ according to

$$\Lambda = \frac{\Gamma_{salt}}{\Sigma_F / F} = \tanh\frac{\Delta\phi_d}{2} \quad (4)$$

when the initial and final concentration $c_{salt,outside}$ are the same, as in the present experimental approach. It must be realized that Eqs. 3 and 4 assume symmetry: the double layer structure in the cathode is equal to that in the anode, except for the difference in the sign of charge; thus μ_{att} must be the same for the cation and the anion. More general models including differences in μ_{att}, as well as the natural charge of the carbon (dependent on local pH) and pseudo-capacitance effects (e.g., the quinone to hydroquinone transition of oxidized carbons) can be developed. Finally, for equilibrium, the applied cell voltage V_{cell}, relates to $\Delta\phi_d$ and $\Delta\phi_{St}$ according to $V_{cell}=2\cdot RT/F\cdot(\Delta\phi_d+\Delta\phi_{St})$.

We use the mD-model to fit to the data in Fig. 2b and Fig. 4, using as input the sub-1nm-micropore volume of Fig. 2a (except for AC-2, for which 0.29 ml/g is used), which multiplied by 85%, gives us the volume/mass parameter, υ. We fit the data using μ_{att}=3.0 kT for all materials, and use for the volumetric Stern layer capacity, $C_{St,vol}$, the empirical expression $C_{St,vol}=C_{St,vol,0}+\alpha\cdot c_{charge,pore}^{2}$, with $C_{St,vol,0}$=200 MF/m^3 for both CDCs and for AC-1, and $C_{St,vol,0}$=190 MF/m^3 for AC-2. We set α=21.7 F·m^3/mol^2 for both CDCs, and α=19.2 F·m^3/mol^2 for both ACs. The use of non-zero values of α is necessary to obtain a good fit to the data, and can be rationalized as being due to a reduction in the closest-approach-distance of the ions to the carbon matrix at higher charge, due to the higher attractive force acting across the Stern layer.[57,58] Note that the fit is still not perfect, and that we have only considered data at c_{salt}=5 mM. Using the same parameter settings, it may be that data at other values of c_{salt} will be described less accurately. Clearly, much work is still to be done in developing accurate EDL models which describe (and fit data for) salt adsorption and charge in microporous carbon electrodes.

For charge efficiency Λ, the four fit curves (one for each material) almost overlap and only one is shown in Fig. 2b. An interesting aspect of the mD-model is that it allows us to make a guess for the amount of counterions and coions in the pores < 1 nm. At 5 mM salt concentration, and for μ_{att}=3 kT, then at zero charge (i.e., before applying a voltage) a micropore ion concentration of 100 mM is predicted for each type of ion. Increasing the cell voltage to V_{cell}=1.4 V, we estimate for CDC-1 that there is a concentration of ~6 mM of the coions left (thus a depletion of 95 mM), while for the counterions the concentration is $c_{counterion,micropores}$=1.7 M. For comparison, the total ion concentration of sea water is about 1 M.

5. Conclusions

In conclusion, we have compared CDC with state-of-the-art commercially available activated carbons and demonstrated that two CDC-powders tested for capacitive deionization (CDI) have significantly higher salt adsorption capacity in the relevant voltage window of 1.2-1.4 V cell voltage at a salt concentration of 5 mM. These results show the potential of CDC-based electrodes for energy-efficient water desalination, and stress the importance of pore size control for achieving optimized salt adsorption capacity. For the various porous carbon materials tested, we find more or less equal values for the charge efficiency, which is the equilibrium ratio of salt adsorption over charge, indicating that materials that show good performance for supercapacitors, may also be very suitable for CDI.

Acknowledgments

Part of this work was performed in the TTIW-cooperation framework of Wetsus, Centre of Excellence for Sustainable Water Technology (www.wetsus.nl). Wetsus is funded by the Dutch Ministry of Economic Affairs, the European Union Regional Development Fund, the Province of Friesland, the City of Leeuwarden and the EZ/Kompas program of the "Samenwerkingsverband Noord-Nederland." We thank the members of the themes “Capacitive Deionization” and “Advanced Waste Water Treatment” in Wetsus for their participation in this research. Y.G. was partially supported by the US National Science Foundation (award number ICC-0924570). R.D. and L.W. would like to thank Dr. Theodore Scabarozi, Oleksandr Kramarenko and Bojanna Shan-theyanda for helpful discussions.

References

1. Seckler, D.; Molden, D.; Barker, R.; International Water Management Institute **1999**, http://pdf.usaid.gov/pdf_docs/PNACH595.pdf.
2. Service, R.F. *Science* **2006**, *313*, 1088.
3. Greenlee, L.F.; Lawler, D.F.; Freeman, B.D.; Marrot, B.; Moulin, P. *Water Research* **2009**, *43*, 2317.
4. Shannon, M.A.; Bohn, P.W.; Elimelech, M.; Georgiadis, J.G.; Mariñas, B.J.; Mayes, A.M. *Nature* **2008**, *452*, 301.
5. Semiat, R. *Env. Sci. Techn.* **2008**, *42*, 8193.
6. Schiermeier, Q. *Nature* **2008**, *452*, 260.
7. Micale, G.; Cipollina A.; Rizzuti, L. *Seawater Desalination: Conventional and Renewable Energy Processes*; Springer, Berlin, 2009.
8. Humplik, T.; Lee, J.; O'Hern, S.C.; Fellman, B.A.; Baig, M.A.; Hassan, S.F.; Atieh, M.A.; Rahman, F.; Laoui, T.; Karnik, R.; and Wang. E. N.; *Nanotechnology* **2011**, *22*, art.no. 292001.
9. Elimelech, M.; Phillip, W.A., *Science*, **2011**, *333*, 712-717.
10. Biesheuvel, P.M. *J. Colloid Interface Sci.* **2009**, *332*, 258.
11. Strathmann, H. *Ion-Exchange Membrane Separation Processes*; Elsevier, Amsterdam, 2004.
12. Sonin, A.A.; Probstein, R.F. *Desalination* **1968**, *5*, 293.
13. Kim, S.J.; Ko, S.H.; Kang, K.H.; Han, J. *Nature Nanotechn.* **2010**, *5*, 297.
14. Pasta, M.; Wessells, C.D.; Cui, Y.; La Mantia, F. *Nano Letters* **2012**, 10.1021/nl203889e
15. Blair, J.W.; Murphy, G.W. *Adv. Chem. Ser.* **1960**, *27*, 206.
16. Murphy, G.W.; Caudle, D.D. *Electrochimica Acta* **1967**, *12*, 1655.
17. Johnson, A.M.; Newman, J. *J. Electrochem. Soc.* **1971**, *118*, 510.
18. Oren, Y.; Soffer, A. *J. Appl. Electrochem.* **1983**, *13*, 473.
19. Farmer, J.C.; Fix, D.V.; Mack, G.V.; Pekala, R.W.; Poco, J.F. *J. Electrochem. Soc.* **1996**, *143*, 159.
20. Yang, K.-L.; Ying, T.-Y.; Yiacoumi, S.; Tsouris, C.; Vittoratos, E.S. *Langmuir* **2001**, *17*, 1961.
21. Gabelich, C.J.; Tran, T.D.; Mel Suffet, I.H. *Env. Sci. Techn.* **2002**, *36*, 3010.
22. Welgemoed, T.J.; Schutte, C.F. *Desalination* **2005**, *183*, 327.
23. Xu, P.; Drewes, J.E.; Heil, D.; Wang, G. *Water Research* **2008**, *42*, 2605.
24. Biesheuvel, P.M.; Van Limpt, B.; Van der Wal, A. *J. Phys. Chem. C* **2009**, *113*, 5636.

25. Noked, M.; Avraham, E.; Soffer, A.; Aurbach, D. *J. Phys. Chem. C* **2009**, *113*, 21319.
26. Bouhadana, Y.; Avraham, E.; Soffer, A.; Aurbach, D. *AIChE J.* **2010**, *56*, 779.
27. Zhao, R.; Biesheuvel, P.M.; Miedema, H.; Bruning, H.; Van der Wal, A. *J. Phys. Chem. Lett.* **2010**, *1*, 205.
28. Lee, J.B.; Park, K.K.; Eum, H.M.; Lee, C.W. *Desalination* **2006**, *196*, 125.
29. Li, H.; Gao, Y.; Pan, L.; Zhang, Y.; Chen, Y.; Sun, Z. *Water Research* **2008**, *42*, 4923.
30. Biesheuvel, P.M.; Van der Wal, A. *J. Membrane Sci.* **2010**, *346*, 256.
31. Kim, Y.-J.; Choi, J.-H. *Water Res*. **2010**, 44, 990.
32. Biesheuvel, P.M.; Zhao, R.; Porada, S.; Van der Wal, A. *J. Colloid Interface Sci.* **2011**, *360*, 239.
33. Li H.; Zou, L.; *Desalination* **2011**, *275*, 62.
34. Ying, T.-Y.; Yang, K.-L.; Yiacoumi, S.; Tsouris, C. *J. Colloid Interface Sci.* **2002**, *250*, 18.
35. Jung, H.-H.; Hwang, S.-W.; Hyun, S.-H.; Lee, K.-H.; Kim, G.-T. *Desalination* **2007**, *216*, 377.
36. Biener, J.; Stadermann, M.; Suss, M.; Worsley, M.A.; Biener, M.M.; Rose K.A.; Baumann, Th.F. *Energy & Env. Sci.* **2011**, *4*, 656.
37. Zou, L.; Morris, G.; Qi, D. *Desalination* **2008**, *225*, 329.
38. Ryoo, M.-W.; Seo, G. *Water Research* **2003**, *37*, 1527.
39. Oh, H.-J.; Lee, J.-H.; Ahn, H.-J.; Jeong, Y.; Kim, Y.-J.; Chi, Ch.-S. *Thin Solid Films* **2006**, *515*, 220.
40. Li, H.; Zou, L.; Pan, L.; Sun, Z. *Environ. Sci. Technol.* **2010**, *44*, 8692.
41. Dai, K.; Shi, L.; Fang, J.; Zhang, D.; Yu, B. *Materials Letters* **2005**, *59*, 1989.
42. Li, H.; Gao, Y.; Pan, L.; Zhang, Y.; Chen, Y.; Sun, Z. *Water Research* **2008**, *42*, 4923.
43. Presser, V.; Heon, M.; Gogotsi, Y. *Adv. Funct. Mat.* **2011**, *21*, 810.
44. Chmiola, J.; Yushin, G.; Gogotsi, Y.; Portet, C.; Simon, P.; Taberna, P.L. *Science* **2006**, *313*, 1760.
45. Chmiola, J.; Largeot, C.; Taberna, P.-L.; Simon, P.; Gogotsi, Y. *Science* **2010**, *328*, 480.
46. Presser, V.; McDonough, J.; Yeon, S.-H.; Gogotsi, Y. *Energy Environ. Sci.* **2011**, *4*, 3059.
47. Dash, R.; Chmiola, J.; Yushin, G.; Gogotsi, Y.; Laudisio, G.; Singer, J.; Fischer, J.E.; Kucheyev, S. *Carbon* **2006**, *44*, 2489.
48. Jagiello, J.; Oliver, J.P. *J. Phys. Chem. C* **2009**, *113*, 19382.
49. Lim, J.-A.; Park, N.-S.; Park, J.-S.; Choi, J.-H. *Desalination* **2009**, *238*, 37.
50. Soffer, A.; Folman, M. *Electroanal. Chem*. **1972**, *38*, 25.
51. Avraham, E.; Bouhadana, Y.; Soffer, A.; Aurbach, D. *J. Electrochem. Soc.* **2009**, *156*, P95.
52. Feng, G.; Qiao, R.; Huang, J.; Sumpter, B.G.; Meunier, V. *ACS Nano* **2010**, *4*, 2382.
53. Kastening, B.; Heins, M. *Electrochimica Acta* **2005**, *50*, 2487.
54. Biesheuvel, P.M.; Bazant, M.Z. *Phys. Rev. E* **2010**, *81*, 031502.
55. Biesheuvel, P.M.; Fu, Y.; Bazant, M.Z. *Phys. Rev. E* **2011**, *82*, 061507.
56. Arafat, H.A.; Franz, M.; Pinto, N.G. *Langmuir* **1999**, *15*, 5997.
57. Grahame, D.C. *Chem. Rev.* **1947**, *41*, 441.
58. Bazant, M.Z.; Chu, K.T.; Bayly, B.J. *SIAM J. Appl. Math.* **2005**, *65*, 1463.

TOC-picture

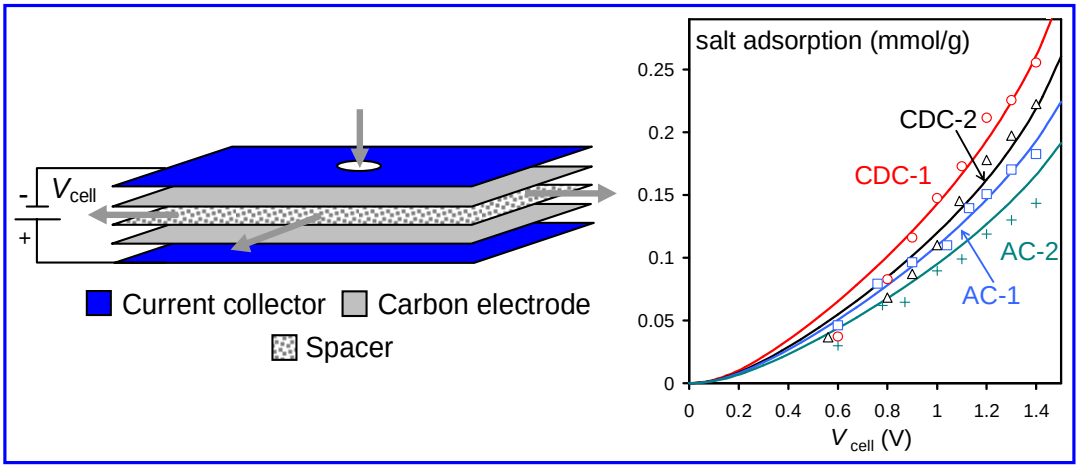
-
V_{cell}
+
Current collector
Carbon electrode
Spacer
salt adsorption (mmol/g)
0.25
0.2
0.15
0.1
0.05
0
0
0.2
0.4
0.6
0.8
1
1.2
1.4
V_{cell} (V)
CDC-2
CDC-1
AC-2
AC-1